Bias-Magnetic Force for Vibration Reduction of Magnetic Bearing Motors

Chien-Chang Wang[1] and Y. D. Yao[1,2]

[1]Materials Science and Engineering, National Chiao Tung University, Hsinchu 300, Taiwan, R.O.C.
[2]Department of Materials Engineering, Tatung University, Taipei 104, Taiwan, R.O.C.

The objective of this paper is to propose a compact method using a novel bias magnet to induce an axial bias-magnetic force in order to reduce the radial vibration of a magnetic bearing (MB) motor. After applying the bias-magnetic force, the optimal radial vibration of the developed MB motor is only around 0.197 g (peak–peak, $1\ g = 9.8$ m/s^2) when the natural frequency of the bias magnet reaches the resonant frequency of 62 Hz. In this optimal condition, the ratio in the radial vibration of the MB motor with the bias-magnetic force to the original one is around 89%, and the driving power of 0.24 W is saved.

Index Terms—**Bias-magnetic force, magnetic bearing (MB), radial vibration, preload.**

I. INTRODUCTION

PASSIVE magnetic bearing (MB) motors present good potential for using in high efficiency, low power consumption, and extremely high-speed devices such as hard disk drive spindle motors, optical disc drives, and fan motors [1], [2], etc. In the design of the MB motor, it is crucial to design adequate axial stiffness of the MB for maintaining the minimum mechanical friction loss below a specified level and for minimizing the radial vibration due to the dynamic rotor system. However, many studies [3], [4] have been focused on the MB motor design, but little research has been done on the reduction of the radial vibration by considering the control of the axial force.

In this paper, the axial forces composed of the preload, wind force, and bias-magnetic force are reported by both finite-element analysis (FEA) and experimental measurement. The variation of radial vibration of the developed spindle motor is determined as a function of the effectiveness of axial force.

II. DESIGN AND FORCE CALCULATION

Fig. 1 shows the MB motor with a bias magnet. The motor consists of a spindle motor, an MB system, a PCB, and a Base. The motor has four slots and four poles. The radial air gap between the stator and magnet made of Ba-ferrite with an inner radius of 1.57×10^{-2} m, axial length of 1.34×10^{-2} m, and a radial thickness of 2×10^{-3} m is designed to be 7×10^{-4} m. Outside the ferrite ring, an iron yoke with a radial thickness of 8×10^{-4} m is mounted. The principle electrical parameters for the MB motor are 3720 rpm under a current of 0.27 A. The MB system consists of two MB units assembled in lower and upper end of the shaft, and separated by an axial length of 7.5×10^{-3} m. Each unit designed with a radial air gap of 5×10^{-4} m and bearing length of 4×10^{-3} m consists of one inner and outer ring magnet made of Nd–Fe–B with $(BH)_{max}$ of 45 MGOes, and magnetized in the same axial direction along the shaft. The inner ring with an inner diameter of 3×10^{-3} m is rotated with the shaft, and the outer one is fixed on the stator. Both of these two rings are designed with the identical radial thickness of 1.5×10^{-3} m. In order to generate the adequate radial restoring force to support the radial load, the geometry of the MB system has been optimally designed. Therefore, the MB can stably maintain the slight radial air gap between the rotating and stationary parts of the motor. However, to avoid the inherent stability problem [5], a single conjunctive pivot point is employed between the shaft and the thrust plate.

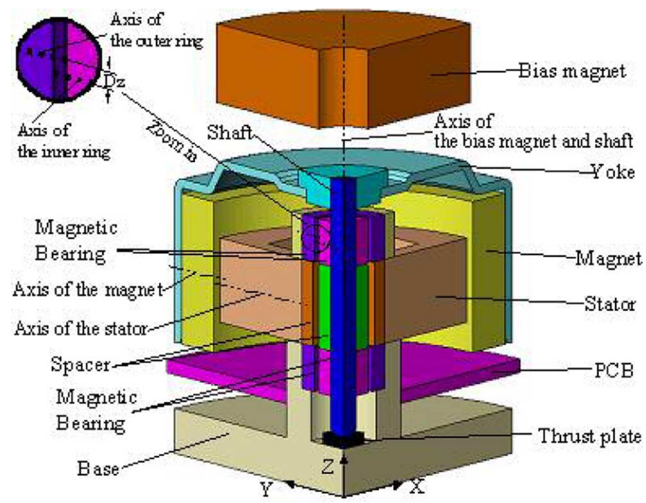

Fig. 1. Schematic of the MB motor with a bias magnet.

The novel bias-magnet made of $(BH)_{max}$ of 33 MGOes with an outer diameter of 3.09×10^{-4} m, inner diameter of 6×10^{-3} m, and axial length of 7×10^{-3} m is employed above the motor as a dynamic vibration absorber [6].

To calculate these axial forces, FEA software of MAGNET 6.18 is applied First, we estimate the downward force. This force, called preload, is the axial force generated due to the offset axis displacement between the stator and magnet. Also, the offset axis displacement between the inner and outer ring of the MB unit contributes to it (see Fig. 1). To compute the force, the rotor is shifted along the negative Z-axis with a displacement interval of 5×10^{-5} m when the Dz ranges from zero (the balanced position) to 4×10^{-4} m. The Dz is the axial gap between the lateral axis of the inner and outer ring magnet of the MB unit (see enlargement top left in Fig. 1). After performing the FEA calculation, the preload as a function of the Dz can be

Digital Object Identifier 10.1109/TMAG.2007.893776

Color versions of one or more of the figures in this paper are available online at http://ieeexplore.ieee.org.

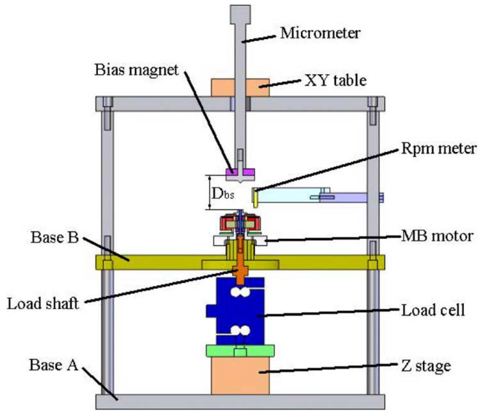

Fig. 2. Configuration of the test setup for axial force measurement.

gained. Second, we compute the upward force. This force consists of bias-magnetic force and wind force. For determining the bias-magnetic force, the bias magnet with the same axis of the shaft is arranged above the MB motor, and the axial distance from the top surface of the shaft to the bottom surface of the bias magnet corresponds to $D_{\rm bs}$ (see Fig. 2). When the $D_{\rm bs}$ ranges from 1.77×10^{-2} to 5.27×10^{-2} m, the bias magnet is shifted along the positive Z-axis with a displacement interval of 5×10^{-3} m, so the bias-magnetic force which varies with the $D_{\rm bs}$ is successfully estimated subtracting the net axial force from preload. The wind force is determined by an experimental approach, and is supposed to be independent of the Dz or $D_{\rm bs}$. Since the downward and upward forces are estimated, the calculation of the net axial force of the proposed system in the dynamic state can be completely performed.

III. Experiment and Results

Fig. 2 shows the configuration of the test setup for the axial force measurement. The MB motor supported by a load shaft with a single conjunction point is fixed on a Base B that is tightly fixed to a Base A. The load shaft is locked to a load cell used to measure the axial force, and fixed to a z stage. For applying a bias-magnetic force to the motor, the bias magnet is fixed to a micrometer locked to an xy table. Then the table is assembled to a Base B. The running speed and current of the motor are collected from power supply and RPM meter, respectively. After the desired forces are completely measured, the MB motor is reassembled with a base, and an accelerometer is attached to the base of the motor in the radial direction to record the radial vibration.

The mean value of measured wind force of the motor is around 0.596 N upward. The predicted preload of the motor is compared with experimental preload, as shown in Fig. 3(a). Fig. 3(b) displays the comparison of predicted net axial force of the motor in dynamic state with experimental net axial force. Since these three axial forces discussed above are determined, the bias-magnetic force of the motor can be successfully calculated deducting the wind force and preload from the net axial force, as shown in Fig. 3(c). For effectively achieving the radial vibration reduction of the motor, the distribution of the bias-magnetic force as a function of the $D_{\rm bs}$ is specially

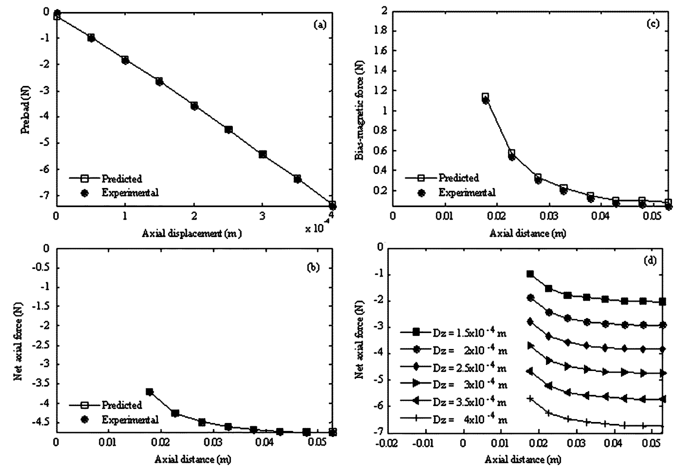

Fig. 3. (a) Comparison of predicted preload of the MB motor with experimental preload. (b) Comparison of predicted net axial force of the MB motor with experimental net axial force. (c) Comparison of predicted bias-magnetic force of the MB motor and experimental bias-magnetic force. (d) Measured net axial force of the MB motor with bias magnetic force for Dz in different positions.

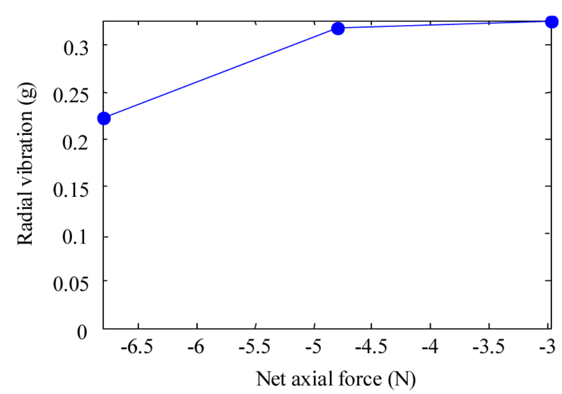

Fig. 4. Radial vibration of the MB motor as a function of the net axial force.

designed, so the frequency of the bias magnet can be exactly tuned to the same frequency as the rated speed of the MB motor. To get the profiles [Fig. 3(b) and (c)], the Dz of the motor is set at 3×10^{-4} m. The above results reveal that predicted axial forces, the net axial and bias-magnetic forces, have good agreement with the experimental data. This suggests that the FEA could be considered utilizing the prediction of the key axial forces, essentially affecting the radial vibration of the developed MB motor. For evaluating the bias-magnetic force effect under the case of the varied preload of the MB motor, the net axial force of the motor in the rotating state is measured corresponding to different positions of Dz, the initial and end positions are 1.5×10^{-4}, and 4×10^{-4} m, respectively, and the sampling interval between the two positions is 5×10^{-5} m, as shown in Fig. 3(d).

Without the bias-magnetic force, the radial vibration of the motor, probed as Dz, is in three different positions, 2×10^{-4}, 3×10^{-4}, and 4×10^{-4} m, as shown in Fig. 4. The related net axial forces of these three concerned positions are -2.981, -4.804, and -6.803 N, respectively. The distribution of the radial vibration as a function of the net axial force indicates that the radial vibration is decreased when the net axial force is increased.

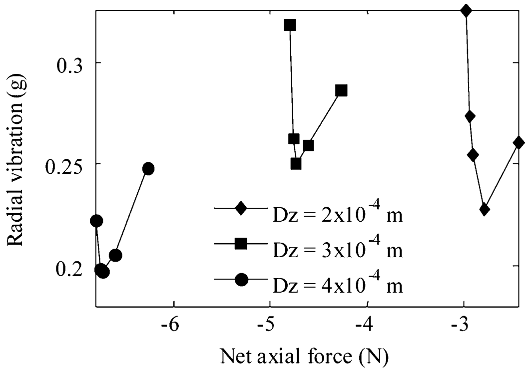

Fig. 5. Radial vibration of the MB motor as a function of the net axial force and Dz.

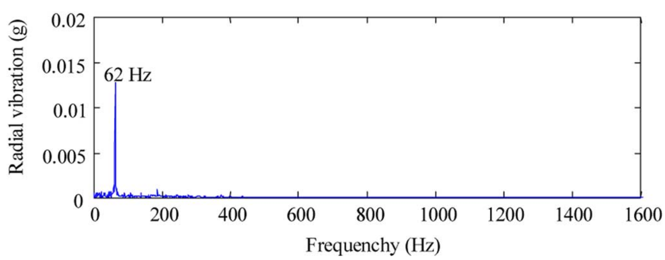

Fig. 6. Dominant magnitude of the radial vibration in frequency domain measured on the bias magnet.

However, when the bias-magnetic force is applied to the MB motor, the radial vibration of the motor can be sharply diminished, as shown in Fig. 5. To investigate the behavior of bias-magnetic force in reducing the radial vibration of the MB motor, the Dz is fixed at three selected positions, $2 \times 10^{-4}, 3 \times 10^{-4}$, and 4×10^{-4} m, then the bias-magnetic force is applied to each condition; however, the point with the maximum net axial force of each individual curve is in the case of the proposed motor without the bias-magnetic force. According to the discussion of Fig. 4, normally the decrease of the net axial force of the MB motor will result in increasing the radial vibration of the motor; however, there exists three local minimum radial vibrations of the MB motor as the net axial force is gradually decreased in each curve (see Fig. 5). This demonstrates that the proper bias-magnetic force distributions generating the exact axial stiffness to make the natural frequency of the bias magnet equivalent to the rotating speed of the MB motor are significantly useful for reducing the radial vibration of the motor. When the motor is operated, and generates these three minimum radial vibration waveforms, each of these dominant magnitudes in the frequency domain corresponding to the waveforms shows the same frequency with the rated rotational speed, 62 Hz, as shown in Fig. 6. Fig. 7(b) shows that the time response of the local optimal radial vibration of the MB motor operated with the bias-magnetic force of 0.539 N and the net axial force of -6.735 N is around 0.197 g (peak–peak), and the ratio in the radial vibration of the MB motor under this condition to the one eliminating the bias force shown in Fig. 7(a) is around 89%, and it saves around 0.24 W of driving power.

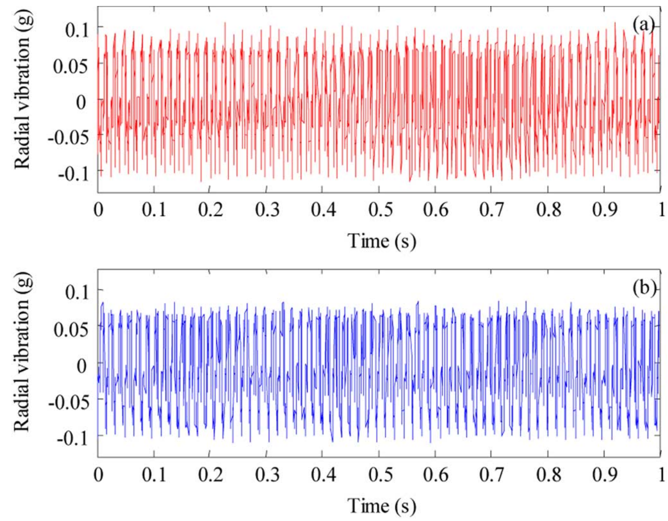

Fig. 7. Time responses of radial vibration of the MB motor (a) without and (b) with bias-magnetic force.

IV. Conclusion

The radial vibration of the MB motor affected by axial force has been investigated. The lower net axial force of the motor can result in increasing the radial vibration of the motor. However, the applied bias-magnetic force contributing to suppressing the axial force of the motor can significantly reduce the radial vibration of the spindle motor when the resonant frequency is reached. Therefore, the bias-magnetic force could be useful for the reduction of the radial vibration of an MB motor. A compact bias-magnetic force device embedded in an MB motor would be implemented in the future work.

Acknowledgment

This work was supported in part by the National Science Council of Taiwan under Grant NSC95-2112-M-001-059.

References

[1] G. H. Jang and J. S. Park, "Development of a highly efficient hard disk drive spindle motor with a passive magnetic thrust bearing and a hydrodynamic journal bearing," *J. Appl. Phys.*, vol. 97, p. 10Q507, May 2005.

[2] C. C. Wang, Y. D. Yao, P. C. Tung, R. B. Xiao, and Y. H. Chang, "Magnetic force-induced damping effect for magnetic bearing motor," *J. Appl. Phys.*, vol. 97, p. 10Q502, May 2005.

[3] J. Delamare, E. Rulliere, and J. P. Yonnet, "Classification and synthesis of permanent magnet bearing configurations," *IEEE Trans. Magn.*, vol. 31, no. 6, pt. 2, pp. 4190–4192, Nov. 1995.

[4] V. Fernandez, J. Fandino, C. Sauvey, J. P. Yonnet, G. Reyne, and O. Cugat, "A design methodology for permanent magnet microbearings," *IEEE Trans. Magn.*, vol. 36, no. 4, pt. 1, pp. 1919–1922, Jul. 1995.

[5] S. Earnshaw, "On the nature of the molecular forces which regulate the constitution of the luminiferous ether," *Phil. Trans. Camb. Soc.*, vol. 7, pp. 97–112, 1842, London.

[6] C. M. Harris, *Shock and Vibration Handbook*, 4th ed. New York: McGraw-Hill, 1995, pp. 6.4–6.9.

Manuscript received October 31, 2006 (e-mail: ydyao@phys.sinica.edu.tw).